Electronic Supplementary Material (ESI) for Inorganic Chemistry Frontiers.

The effect of Sc doping on the electrocatalytic and optoelectronic properties of 2D SiAs single crystal

Tong Yu [a], Qiubo Chen [b], Hailong Qiu*[a], Hongjun Liu [a], Zhanggui Hu [a] and Yicheng Wu [a]

Supporting Information

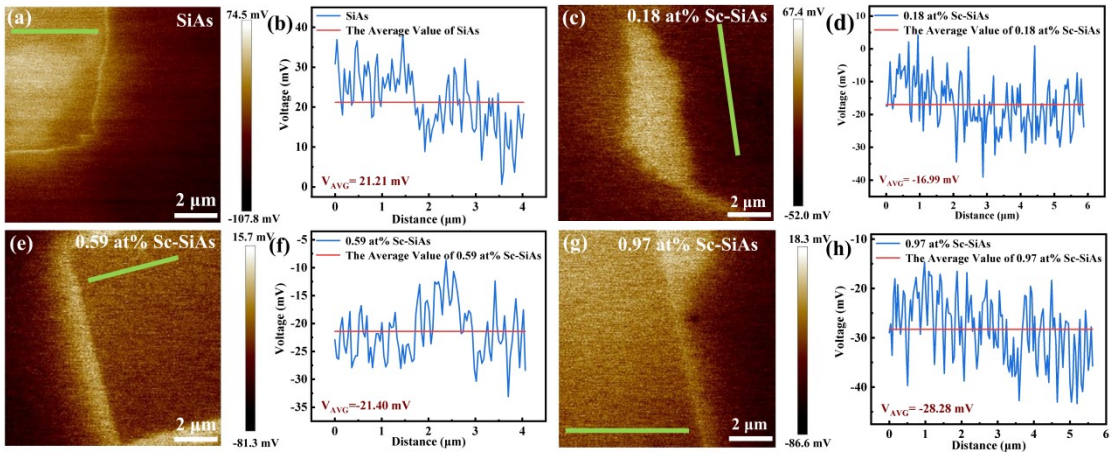

Fig. S1 KPFM images and the measured contact potential difference of the mechanically exfoliated (a,b) pristine SiAs, (c,d) 0.18 at% Sc-SiAs, (e,f) 0.59 at% Sc-SiAs, and (g,h) 0.97 at% Sc-SiAs few layers.

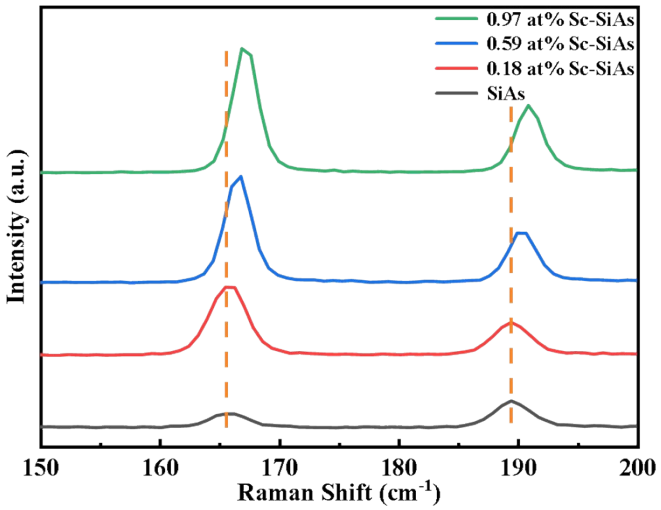

Fig. S2 Raman spectroscopy of the Sc-doped SiAs synthesized by CVT method.

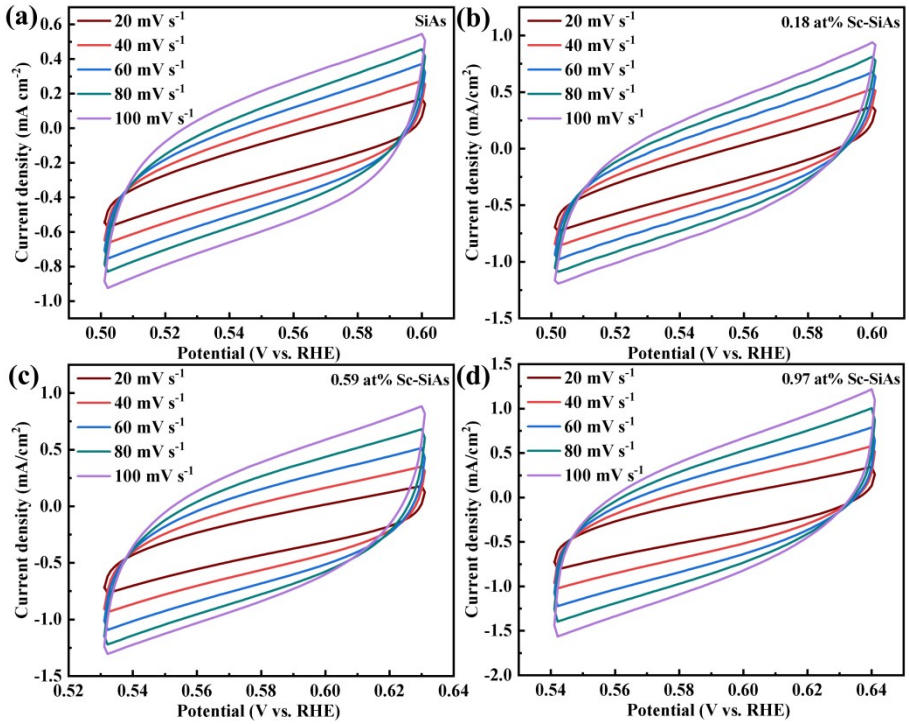

Fig. S3 Cyclic voltammetry curves of (a) SiAs, (b) 0.18 at% Sc-SiAs, (c) 0.59 at% Sc-SiAs, (d) 0.97 at% Sc-SiAs samples at various scan rates from 20 to 100 mV/s in 0.5 M H_2SO_4.

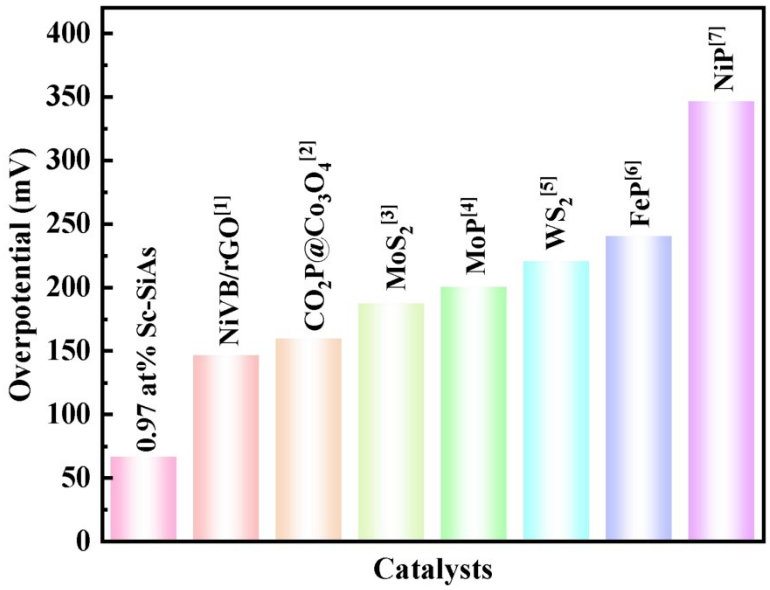

Fig. S4 The overpotential of 0.97 at% Sc-SiAs and other catalysts with current density of 10 mA/cm^2 is compared.

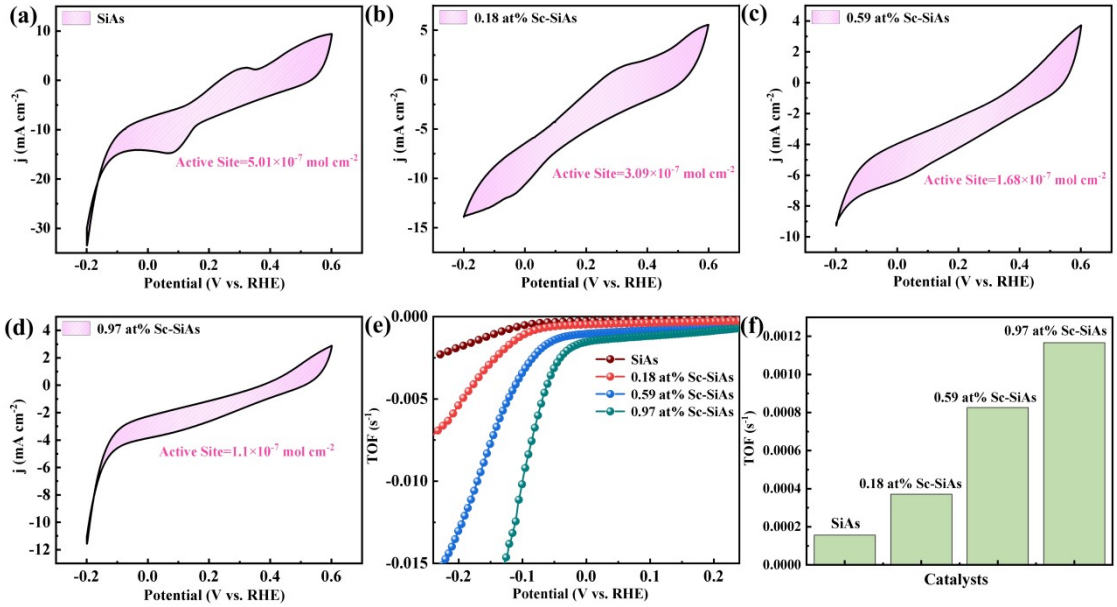

Fig. S5 Cyclic voltammetry curves of (a) SiAs, (b) 0.18 at% Sc-SiAs, (c) 0.59 at% Sc-SiAs, (d) 0.97 at% Sc-SiAs samples in 0.5 M H_2SO_4 with scan rate of 50 mV/s. (e) Calculated TOF of SiAs and Sc-doped SiAs in acid solution. (f) Comparison of TOF values of SiAs and Sc-doped SiAs at an overpotential of 100 mV.

To calculate turnover frequency (TOF), CV method with the potential range of -0.2 to 0.6 V (vs. RHE) at a scan rate of 50 mV/s was performed in 0.5 M H_2SO_4. When the number of active sites is determined, the turnover frequency (TOF) is evaluated by the following standard equation [Eq. (1)][8,9]:

$$TOF = (J \times A)/(2 \times F \times n) \quad (1)$$

Where j (A/cm^2) is the current density in LSV curves, A is the surface area of the electrode (0.01 cm^2), F stands for the Faraday constant, the number of 2 represents 2 electrons/mol of H_2, F is the Faraday constant (96500 C/mol), and n stands for the number of moles of C atoms in samples.

The number of active sites was measured from CV curves within the potential range of -0.2 to 0.6 V (vs. RHE) at a scan rate of 50 mV/s in 0.5 M H_2SO_4, as shown in Fig S5(a)-(d). The number of active sites (n) is proportional to the integral area (S) of the CV curve, satisfying the formula [Eq. (2)]:

$$n = (S \times 10^{-3})/(2 \times \nu \times F) \quad (2)$$

Therefore, the relationship between TOF and Potential is calculated according to the above formula, as shown in Fig S5(e). Fig S5 (f) shows the TOF values of SiAs, 0.18 at% Sc-SiAs, 0.59 at% Sc-SiAs, and 0.97 at% Sc-SiAs extracted when the overpotential is 100 mV. It can be clearly observed that the TOF value of each active site of 0.97 at% Sc-SiAs was 7.5 times that of undoped SiAs, indicating that 0.97 at% Sc-SiAs had higher catalytic activity for HER.

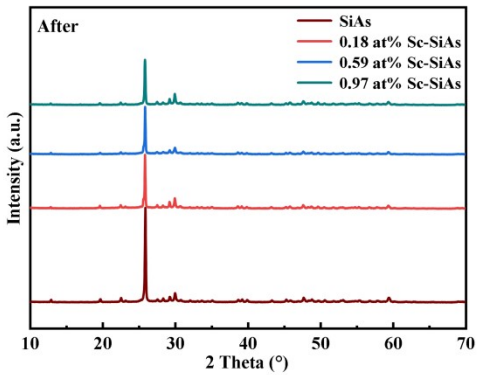

Fig S6 XRD spectrum of undoped SiAs and Sc-SiAs with different Sc doping concentrations after electrocatalytic reaction.

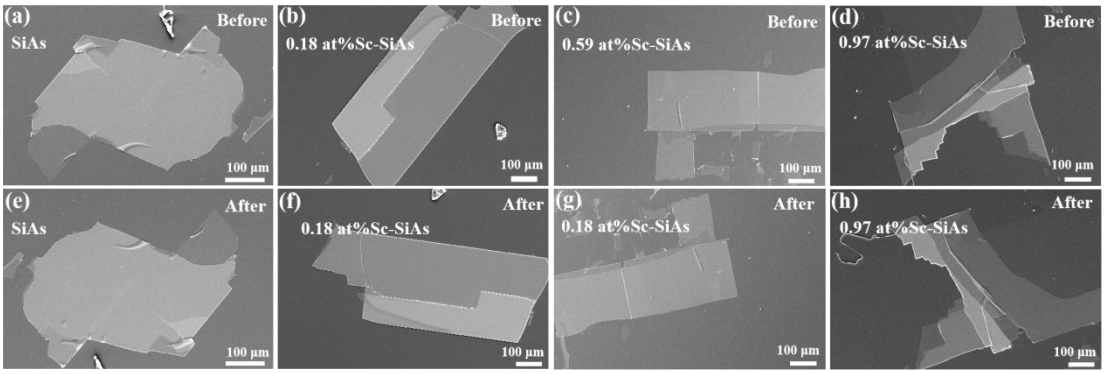

Fig S7 SEM images of four catalysts before and after electrocatalytic reaction, (a, e) SiAs, (b, f) 0.18 at% Sc-SiAs, (c, g) 0.59 at% Sc-SiAs, (d, h) 0.97 at% Sc-SiAs.

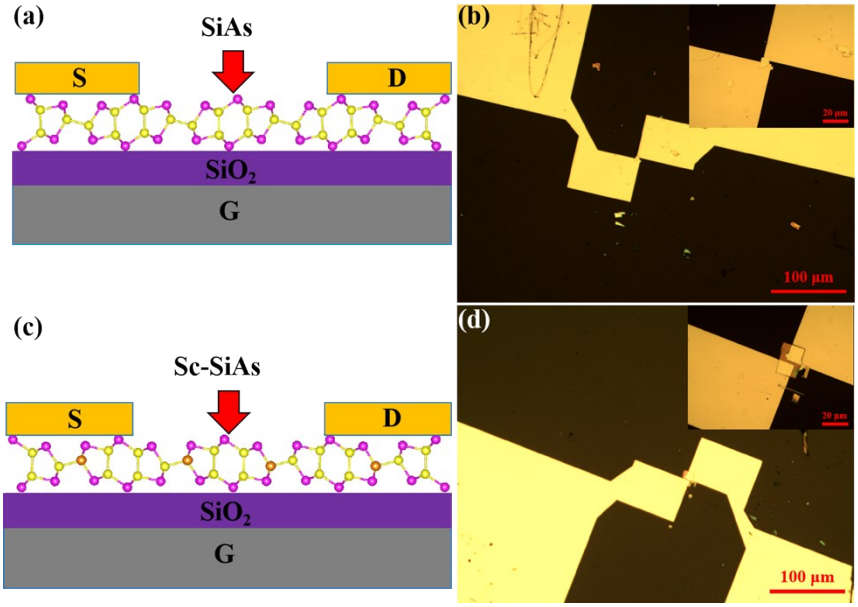

Fig. S8 （a, c）ematic diagram of SiAs and Sc-SiAs device configuration. (b,d) Optical image of a typically fabricated device.

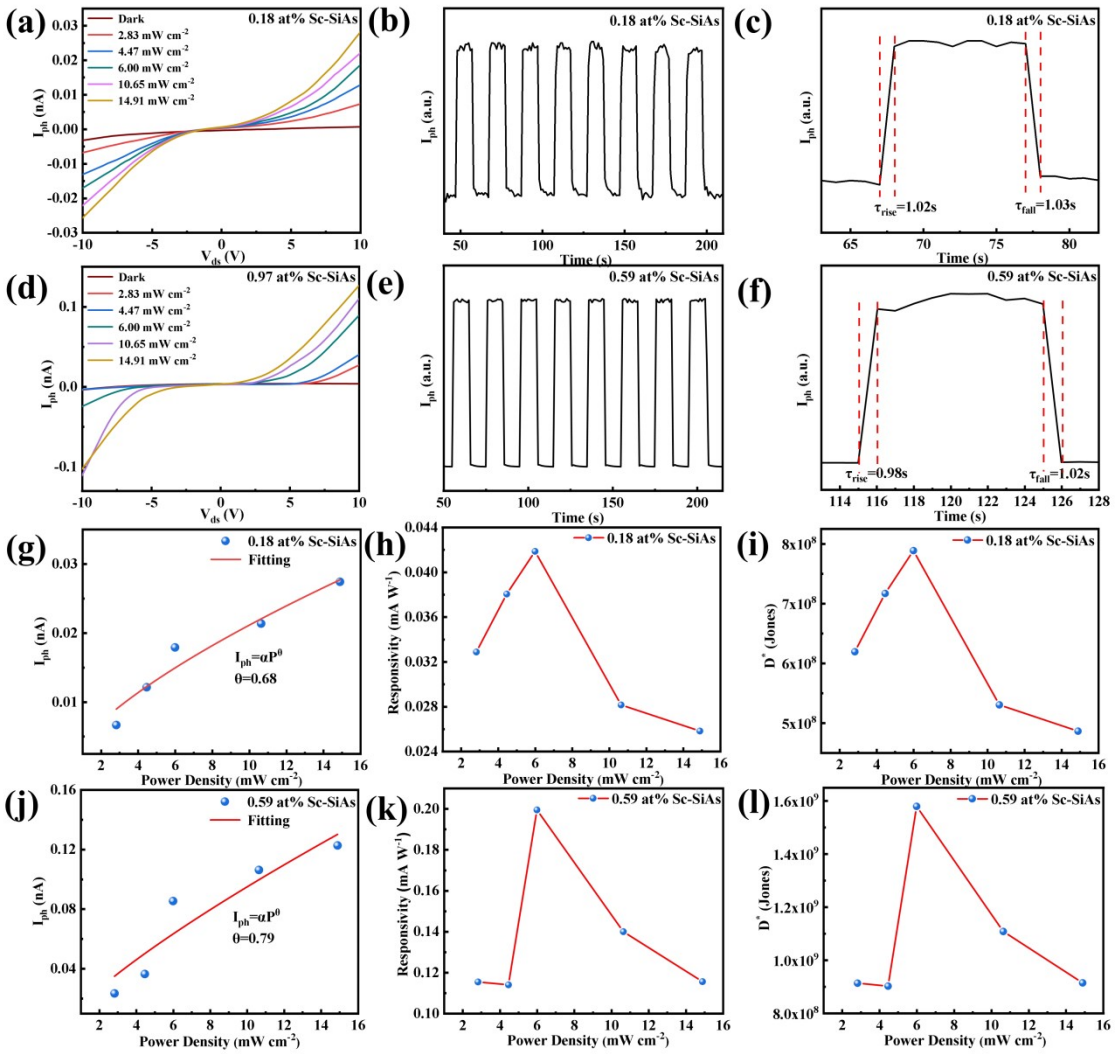

Fig. S9 Optoelectronic performance of photodetectors based on 0.18 at% Sc-SiAs and 0.59 at% Sc-SiAs few layers. (a,d) I-V curves of the device under 550 nm laser illumination with different intensities. (b,e) Time-resolved light response of photodetector at λ=550 nm and Vds=10 V. (c,f) Rising and falling time of the photodetectors. (g,j) Photocurrent as a function of optical power density. (h,k) The relationship between Responsivity and incident optical power. (i,l) The curve of detectivity and laser power density.

1. M. Arif, G. Yasin, M. Shakeel, M. Mushtaq, W. Ye, X. Fang, S. Ji and D. Yan, Highly active sites of NiVB nanoparticles dispersed onto graphene nanosheets towards

efficient and pH-universal overall water splitting, *J. Energy Chem.*, 2021, **58**, 237-246.
2. L. Yao, N. Zhang, Y. Wang, Y. Ni, D. Yan and C. Hu, Facile formation of 2D $Co_2P@Co_3O_4$ microsheets through in-situ toptactic conversion and surface corrosion: Bifunctional electrocatalysts towards overall water splitting, *J. Power Sources*, 2018, **374**, 142-148.
3. M. A. Lukowski, A. S. Daniel, F. Meng, A. Forticaux, L. Li and S. Jin, Enhanced hydrogen evolution catalysis from chemically exfoliated metallic MoS_2 nanosheets, *J. Am. Chem. Soc.*, 2013, **135**, 10274-10277.
4. W. Cui, Q. Liu, Z. Xing, A. M. Asiri, K. A. Alamry and X. Sun, MoP nanosheets supported on biomass-derived carbon flake: One-step facile preparation and application as a novel high-active electrocatalyst toward hydrogen evolution reaction, *Appl. Catal., B*, 2015, **164**, 144-150.
5. D. Voiry, H. Yamaguchi, J. Li, R. Silva, D. C. Alves, T. Fujita, M. Chen, T. Asefa, V. B. Shenoy and G. Eda, Enhanced catalytic activity in strained chemically exfoliated WS_2 nanosheets for hydrogen evolution, *Nat. Mater.*, 2013, **12**, 850-855.
6. Y. Xu, R. Wu, J. Zhang, Y. Shi and B. Zhang, Anion-exchange synthesis of nanoporous FeP nanosheets as electrocatalysts for hydrogen evolution reaction, *Chem. Commun.*, 2013, **49**, 6656-6658.
7. X. Chen, D. Wang, Z. Wang, P. Zhou, Z. Wu and F. Jiang, Molybdenum phosphide: a new highly efficient catalyst for the electrochemical hydrogen evolution reaction, *Chem. Commun.,* 2014, **50**, 11683-11685.
8. W. Gao, M, Yan, H-Y. Cheung, Z. Xia, X. Zhou, Y. Qin, C. Wong, Y. Qu, C. Chang and J. Ho, Modulating electronic structure of CoP electrocatalyst towards enhanced hydrogen evolution by Ce chemical doping in both acidic and basic media, *Nano Energy*, 2017, **38**, 290-296.
9. X. Li, S. Yang, M. Liu, X. Yang, Q. Xu, G, Zeng and Z. Jiang, Catalytic Linkage Engineering of Covalent Organic Frameworks for the Oxygen Reduction Reaction, *Angew. Chem., Int. Ed.*, 2023, **62**, e202304356.